Rheol Acta (2004) 43: 624–633
DOI 10.1007/s00397-004-0359-6

ORIGINAL CONTRIBUTION

Martin Sentmanat
Savvas G. Hatzikiriakos

Mechanism of gross melt fracture elimination in the extrusion of polyethylenes in the presence of boron nitride

Received: 11 December 2003
Accepted: 5 February 2004

M. Sentmanat
Senkhar Technologies, LLC,
Akron, Ohio, USA

S. G. Hatzikiriakos (✉)
Department of Chemical
and Biological Engineering,
The University of British Columbia,
Vancouver, B.C., Canada
E-mail: hatzikir@interchange.ubc.ca

Abstract The mechanism by which the addition of a small amount of boron nitride into a polyethylene eliminates gross melt fracture is elucidated. Simple elongational viscosity measurements at high rates revealed that the presence of boron nitride decreases the extensional viscosity of polyethylenes. The extensional rates at which these effects are present were found to be about the same with those at which gross melt fracture is obtained (calculated from Cogswell's analysis). Thus, it can be argued that the well dispersed boron nitride particles decrease extensional stresses that are responsible for gross melt fracture and/or their presence dissipate the release of energy resulting from isolated rupture or slip planes within the melt originating at the entrance to the capillary.

Keywords Gross melt fracture · Polyethylenes · Boron nitride · Processing aids · Extensional rheometry

Introduction

Flow instabilities such as melt fracture phenomena limit the rate of production in many polymer processing operations including fiber spinning, film blowing, profile extrusion, and various coating flows (Pearson 1985; Larson 1992). In particular, in extrusion processes when the throughput exceeds a critical value, small amplitude periodic distortions appear on the surface of extrudates known as surface melt fracture or sharkskin (Howells and Benbow 1962; Benbow and Lamb 1963; Ramamurthy 1986). At higher throughput rates more severe distortions of irregular form appear known as gross melt fracture (Tordella 1956, 1969). These two phenomena are independent and might occur together. In the gross melt fracture regime, the small amplitude periodic distortions may superpose on the irregular gross distortions. In other words, both phenomena (type of distortions) may be seen together depending on the scale under which they are examined. The surface melt fracture phenomena originate in the land of the die next to the die exit (Cogswell 1972, 1977; Kurtz 1992; Migler et al. 2001, 2002), while gross melt fracture is initiated at the die entry (Tordella 1956, 1969; Bergem 1976; Vinogradov and Malkin 1980; Leonov and Prokunin 1994).

To increase the rate of production by eliminating or postponing the melt fracture phenomena to higher shear rates, processing additives/aids such as fluoropolymers (added at loadings of about 0.1 wt%) may be used. These additives can eliminate only surface (sharkskin) and stick-slip (oscillating or cyclic) melt fracture. They do not appear to have an effect on the extrudate appearance in the gross melt fracture region (Achilleos et al. 2002).

Previous work on eliminating gross melt fracture, have concerned with the role of die geometry (contraction angle) that plays in these phenomena (Bagley and Schreiber 1961; Ballenger et al. 1971). In addition, a filter placed right at the die entrance also has a significant effect by reducing and/or eliminating gross melt fracture to a certain extent (Done et al. 1983; Piau et al.

2000; Goutille and Guillet 2002). It has been recently discovered that certain boron nitride (BN) powders can eliminate gross melt fracture (Buckmaster et al. 1997). The inventors have provided no explanation about the mechanism by which boron nitride eliminates gross melt fracture. This was studied by Kazatchkov et al. (2000) using a visualization technique. They have used a transparent die made out of fused quartz to visualize the change in the flow patterns at the entrance to a capillary die (site of initiation of gross melt fracture) in the presence and absence of a small amount of boron nitride. Long-time exposure photographs were taken at the capillary entry region by using a Nikon FM-2 35 mm photographic camera attached to a microscope (Nikon SMZ-2T). The key features of their study can be summarized as follows. At low shear rates the flow enters the capillary at a higher entry angle, and the vortex in the corner of the reservoir is large. As the shear rate increases, the streamlines bend more near the entrance to the capillary. The vortex also becomes slightly smaller in size because it is suppressed towards the corner by the higher pressure. At high enough shear rates, gross melt fracture is observed, and the streamlines are no longer smooth. In fact, the bulk motion of the melt in the upstream from the entrance region follows a discontinuous motion. The flow in the entry region appears to be broken into several layers, and each layer moves with its own velocity. At regular time intervals, different in each layer, the motion stops for a brief period of time. The closer the layer is towards the center of the stream, the larger and more frequent are the jumps and stops inside it. This flow pattern closely resembles the stick-slip phenomenon observed in the capillary flow of linear polymers. The difference is that the former occurs at multiple polymer surfaces within the bulk of the material, while the latter occurs only close to the polymer-wall interface. Further, it was reported that the addition of 0.1% boron nitride (BN) eliminates the discontinuous layer-like motion even at the highest shear rate of 650 s^{-1}. The streamlines in the presence of boron nitride are smooth, the flow seems to be more organized and the extrudate is free of any distortions. This suggests that BN is a suitable processing aid for eliminating and postponing the onset of gross melt fracture to higher shear rates. It seems that the presence of the BN over the surfaces within the bulk material where stick-slip was observed in its absence, provides proper lubrication between these singular layers (change of stick-slip or intermittent fluid layer motion to a continuous slippage between those fluid layers), thus eliminating stick-slip phenomena within the bulk of the polymer.

In this paper we investigate further the mechanism of gross melt fracture elimination in the presence of BN. It is known that upstream from the entrance region, mixed flow conditions exist (shear and extensional). Studies on gross melt fracture of polyolefins suggest that gross melt fracture originates from this region. It occurs when the extensional stress in this entry region exceeds a critical value (Cogswell 1972, 1977; Kim and Dealy 2002a, 2002b; Hurlimann and Knappe 1972; Shaw 1975; Goutille et al. 2003). Numerical simulations of planar contraction flow with a slip boundary conditions has shown that the azimuthal velocity in the entrance for a Carreau-Yasuda fluid ($n < 0.5$) changes direction, causing significant curvature in the streamlines (Joshi and Denn 2003a, 2003b). The streamline curvature may be relevant to the onset of entry flow instabilities at high stress levels in polymer processing.

Based on these reported findings, we report on measurements of extensional and shear rheological data at conditions similar to those where gross melt fracture occurs. The effect of boron nitride on the extensional rheological data of polyethylenes are related to the effects of boron nitride in their processability as these can be assessed by the onset of gross surface distortions that originate from the high extensional stresses in the entry flow.

Experimental

The experimental results presented in this paper were produced by using two metallocene-catalyzed linear low-density polyethylenes, namely Exact 3128 and Exceed 143 obtained from ExxonMobil. First, the effect of the addition of boron nitride to the polymer on its shear rheology (linear viscoelasticity) was examined by using a Bohlin C-VOR parallel-plate rotational rheometer. The effect of boron nitride on the extensional rheology of Exact 3128 was assessed with the new SER Universal Testing Platform (Sentmanat 2003a, 2003b) from Xpansion Instruments. As depicted in Fig. 1 and further described by Sentmanat (2003a, 2003b) the SER unit is a dual windup extensional rheometer that has been specifically designed for use as a fixture on a variety of commercially available rotational rheometer host platforms. The SER-HV-A01 model used in this study was designed for the ARES rheometer platform and is capable of generating Hencky strain rates up to 20 s^{-1} under controlled temperatures in excess of 250 °C.

A standard Instron piston-driven constant-speed capillary unit was used to assess the processability of this polymer in terms of critical shear rates for the onset of sharkskin, oscillating and gross melt fracture. The usual capillary dies were used in addition to a crosshead die (Nokia Maillefer 4/6) that included dies and tips of various diameters (“tip” is the wire guide) with equal entry cone angles of 60° and the die land length of 7.62 mm. Figure 2 shows a schematic diagram of this cross-head die. The molten polymer enters the die via port [11] and is forced around the wire guide [16] towards the die orifice [8]. The wire guide serves as a mandrel for the molten polymer, giving the extrudate [10] a tubular shape. The die passage [4] forms the exterior surface of the tubular shape, and the exterior surface of the cylindrical extension [24] forms the interior surface of the tubular shape. The greater speed of the wire compared to the polymer extrusion rate causes the polymer coming into contact with the wire at a point remote from the orifice [8] to draw down to a thinner cross-section, forming a thin polymer coating [26] on the wire. This is a melt draw-down extrusion process with a draw down ratio (DDR), which is the ratio of die orifice area to cross-sectional area of the polymer insulation, of at least 5:1. However, in the present study the pressure extrusion makes no use of wire and therefore DDR is irrelevant.

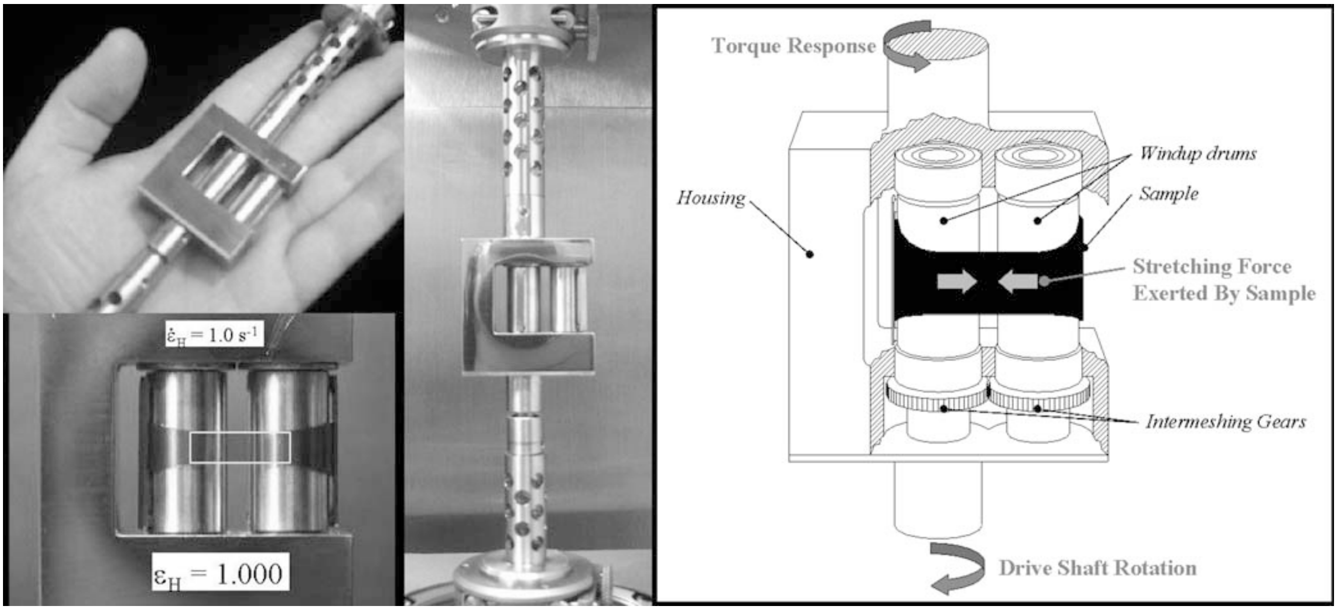

Fig. 1 Photo images of the SER-HV-A01 Universal Testing Platform accommodated on an ARES rotational rheometer host system, and a schematic illustration of the fixture during operation

Two types of boron nitride were used as additives into the resins, namely CTF5 and CTUF. These are similar powders having particle sizes in the range of 10–20 μm with the exception that CTUF has a significant amount of boron oxides (about 2%) that significantly alters its surface chemistry. The surface energy of CTF5 is 47.1 mJ/m^2(35.8 mJ/m^2 and 11.3 mJ/m^2 are the non-polar and polar components respectively) and that of CTUF is 63.4 mJ/m^2(36.9 mJ/m^2 and 26.5 mJ/m^2 are the non-polar and polar component respectively) measured by direct contact angle measurements using polar and non-polar simple liquids (Rathod 2003). It has been reported that CTF5 is an effective additive capable of eliminating both surface and gross melt fracture whereas CTUF fails to eliminate sharkskin melt fracture although it is capable of eliminating gross melt fracture at high rates (Yip et al. 1999, 2000). These were dispersed into the base polymer by first preparing a concentrate of 5 wt%. Consequently, the concentrate was diluted to various final desired concentrations. These final blends were tested in extrusion by using the crosshead die at 100 °C, and 163 °C. Between testing of the various blends, the rheometer was flushed with three full loads of polypropylene in order to purge any remaining BN off the die surface. The extrudates were collected in a cold-water bath in order to freeze their appearance and avoid sagging effects. These were consequently examined carefully to observe distortions on their surface.

The morphology of boron nitride powders as well those of the final blends (to check dispersion) were investigated by using a Hitachi S-2300 Scanning Electron Microscope (SEM) operating at 5 keV. It was observed that both BN powders used had an average particle size of 10–20 μm with medium degree of agglomeration. Finally, the dispersion was found to be uniform which is a requirement for obtaining the best performance of boron nitride in eliminating gross melt fracture phenomena (Yip et al. 1999, 2000).

Linear viscoelastic measurements

It has been reported in the literature that the addition of a small amount of BN has no effect on the linear viscoelastic properties of polymers (Rosenbaum et al. 2000). Figure 3 shows dynamic linear viscoelastic data of pure metallocene-LLDPE (Exact 3128) and m-LLDPE with three different levels of BN (CTF5) at

Fig. 2 A schematic of the crosshead die

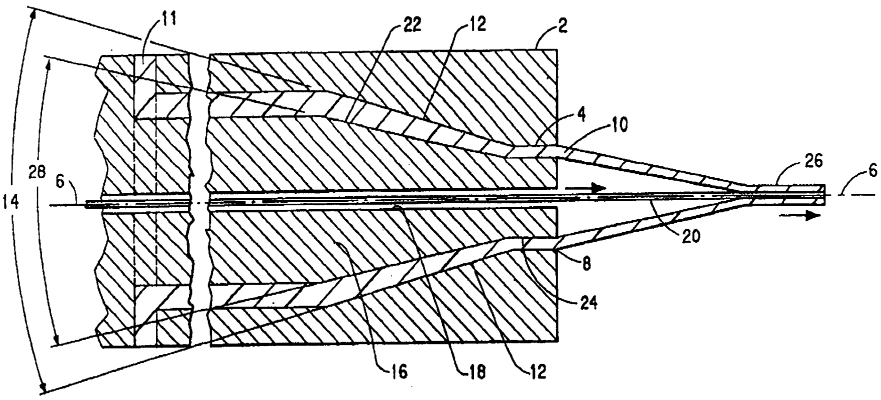

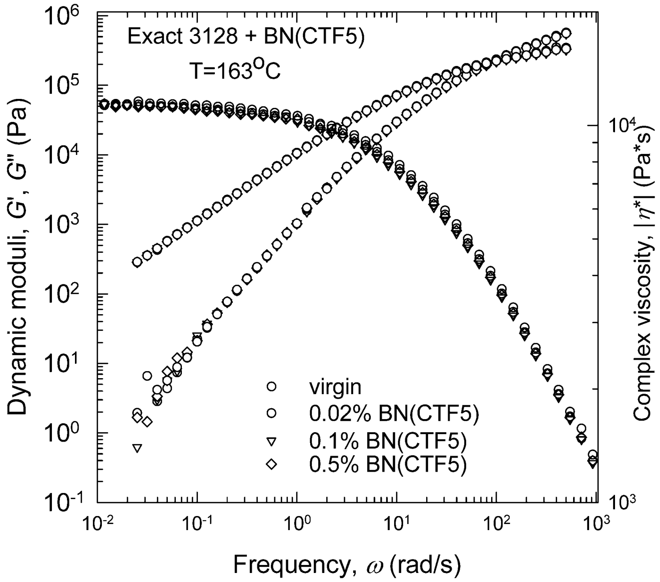

Fig. 3 Linear viscoelastic data for m-LLDPE (Exact 3128) at 163 °C with and without BN

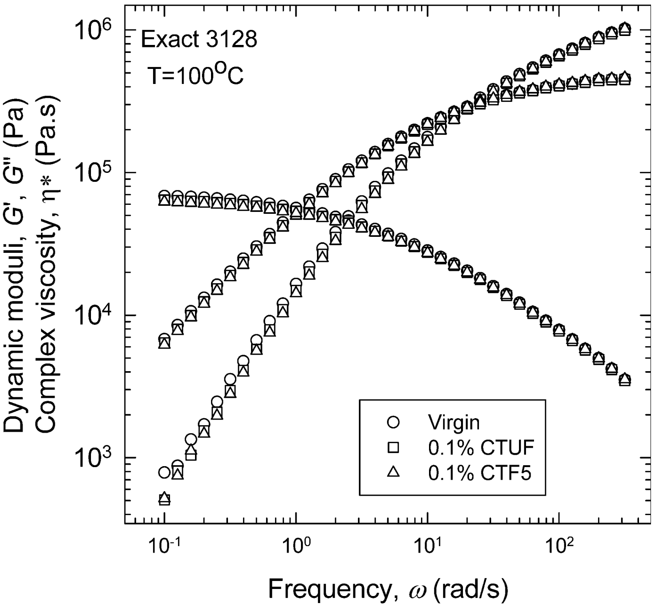

Fig. 4 Linear viscoelastic data for m-LLDPE (Exact 3128) at 100 °C with and without BN (CTF5 and CTUF)

163 °C. No significant difference was found in the linear viscoelastic behavior of pure and filled resins as long as the loadings were kept at relatively low levels (up to 0.5 wt% loadings were examined). Similar results were also obtained at 100 °C. Figure 4 shows the linear viscoelastic behavior of pure m-LLDPE (Exact 3128) and m-LLDPE with 0.1 wt% of two types of BN independently (CTF5 and CTUF). It can be seen that the addition of either CTUF or CTF5 has no effect on the linear viscoelasticity of m-LLDPE (Exact 3128). Additional shear rheological experiments such as stress relaxation after cessation of steady-shear, and large amplitude oscillatory shear have been performed by means of a sliding plate rheometer. Again, no significant differences were detected between the shear rheological data of filled and unfilled resins (including the other m-LLDPE Exceed 143 used in the present work). Similar conclusions have been drawn by Yip (1999), Lee and Lee (2001), and Lee et al. (2000) for several polyolefins and fluoroelastomers. Therefore, shear rheology is not sensitive enough to explain the significant effect of the addition of a small amount of boron nitride on the processability of m-LLDPE (Exact 3128).

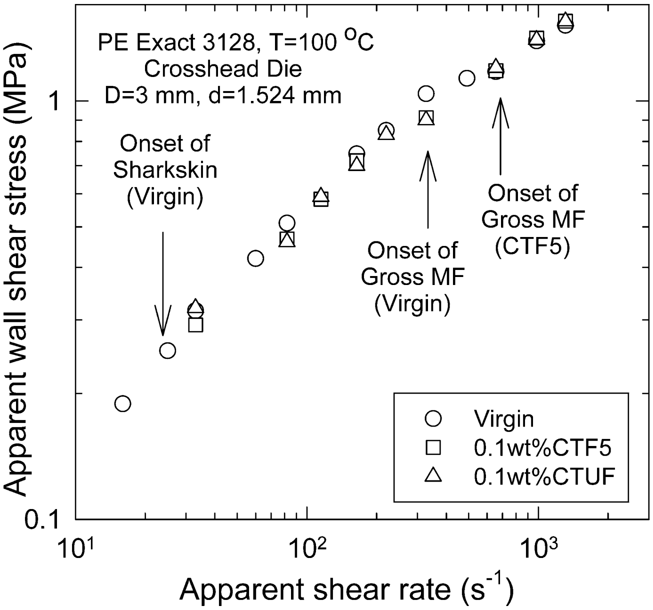

Fig. 5 The effect of BN (CTF5 and CTUF) on the melt fracture behavior of the m-LLDPE (Exact 3128) at 100 °C

Capillary experiments

Figures 5 and 6 depict the flow curves of Exact 3128 with and without BN (CTF5 and CTUF) at 100 °C and 163 °C obtained with a crosshead die attached to the capillary rheometer. The shear stress is plotted as a function of the apparent shear rate. The apparent shear rate was calculated by using the formula applied for slit dies having a large aspect ratio (Bird et al. 1987):

$$\dot{\gamma}_A = \frac{6Q}{0.25(D-d)^2 0.5\pi(D+d)} \tag{1}$$

where Q is the volumetric flow rate, and d and D are the tip and die diameters, correspondingly. The apparent

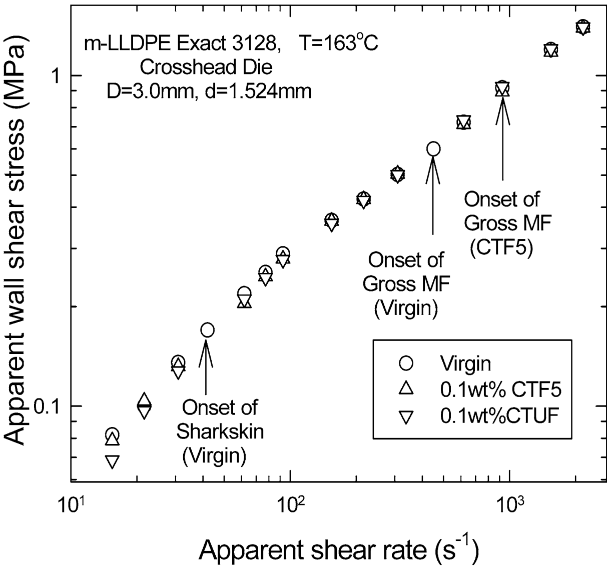

Fig. 6 The effect of BN (CTF5 and CTUF) on the melt fracture behavior of the m-LLDPE (Exact 3128) at 163 °C

wall shear stress was estimated as the average of the shear stress at the inner and outer walls by using the following formula, which is based on the assumption of a power-law fluid (Bird et al. 1987):

$$\tau_{rz} = \frac{\Delta PD}{4L}\left(\frac{2r}{D} - \beta^2 \frac{D}{2r}\right) \qquad (2)$$

where τ_{rz} is the shear stress at radius r, ΔP is the pressure drop, L is the length of the die land, and β is the parameter depending on the geometry and the power law index.

It can be seen from Figs. 5 and 6 that the addition of 0.1 wt% of CTF5 or CTUF has no effect on the flow curve of Exact 3128. However, the presence of boron nitride CTF5 has a striking effect on the processability of Exact 3128. At 100 °C, virgin m-LLDPE (Exact 3128) exhibits sharkskin melt fracture at a critical shear rate of 25 s^{-1} and gross melt fracture at a critical shear rate of 327 s^{-1}. Surprisingly, the addition of CTF5 postpones the onset of gross melt fracture to the critical shear rate of 655 s^{-1}. The addition of CTUF postpones the onset of sharkskin melt fracture to about 80 s^{-1}, although sharkskin persists even at high rates (greater than 327 s^{-1}) where the virgin resin exhibits gross melt fracture. This means that while CTUF is not effective in eliminating sharkskin (die exit/surface phenomenon) due to its high surface energy that prevents its presence at the die wall, it seems to postpone the occurrence of gross melt fracture (bulk phenomenon) at rates comparable to those obtained with CTF5.

Similarly, at 163 °C virgin Exact 3128 exhibits sharkskin melt fracture at a critical shear rate of 42 s^{-1} and gross melt fracture at a critical shear rate of 450 s^{-1}. Surprisingly, the addition of CTF5 postpones the onset of gross melt fracture to the critical shear rate of 928 s^{-1}. The addition of CTUF postpones the onset of sharkskin melt fracture to about 150 s^{-1} although sharkskin persists even at high rates where the virgin resin exhibits gross melt fracture. As discussed above, CTUF is effective for eliminating gross melt fracture but not for sharkskin melt fracture.

As discussed in the introduction, the site of initiation of gross melt fracture is at the entrance region, where significant extensional stresses prevail. A critical extensional stress appears to be the criterion for the onset of gross melt fracture (Cogswell 1972, 1977; Kim and Dealy 2002a, 2002b). Kim and Dealy reported critical extensional stresses for the onset of gross melt fracture of the order of 1–2.5 MPa independent of temperature and molecular weight. These values can be significantly higher for polydisperse polymers having a small degree of long chain branching (Kim and Dealy 2002b). Goutille et al. (2003) have reported a value of 1 MPa for a linear SBR (copolymer of styrene/butadiene rubber) and a value of 1.5 MPa for a branched one.

Based on these reports, it would be logical and relevant at this point to perform simple extensional experiments at high extensional rates in an attempt to reveal possible effects of the addition of boron nitride on the extensional behavior of m-LLDPE (Exact 3128).

Extensional rheological measurements

Figures 7 and 8 plot the tensile stress growth coefficient of pure m-LLDPE (Exact 3128) and m-LLDPE filled with the two types of boron nitride (CTUF and CTF5) in simple extension at 100 °C and 150 °C respectively obtained with the SER rheometer at Hencky strain rates from 0.01 to 20 s^{-1}. Each of the curves was obtained with the use of separate sample specimens that were compression molded into a flat sheet and individually cut to width. As shown in these plots, the superposition of the linear viscoelastic cone and plate results with the tensile stress growth curves at low strains and rates of deformation provides validation of the extensional melt data and a reflection of experimental reproducibility. Note as well how the low rate tensile stress growth data are able to capture the plateau viscosity corresponding to three times the zero-shear viscosity of the polymer melt corresponding to the terminal relaxation zone of linear viscoelastic behavior. Returning to Figs. 7 and 8, it can be seen that at small extensional rates the stress growth curves are identical irrespective of the presence/absence of boron nitride. However, significant differences appear at higher extensional rates, namely at the rates of 10 s^{-1} and 20 s^{-1} that coincide with the rubbery plateau regime of viscoelastic behavior. These differ-

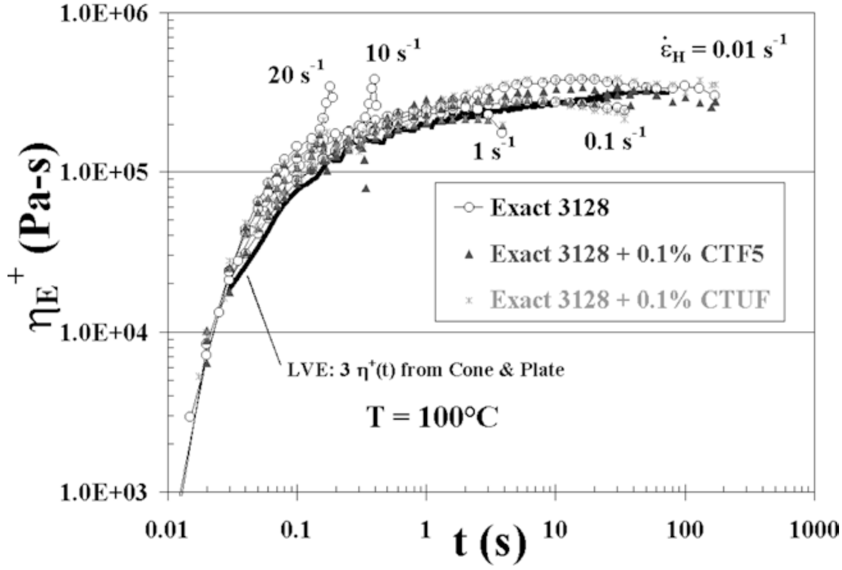

Fig. 7 Tensile stress growth coefficient of boron nitride (CTF5 and CTUF) filled and unfilled m-LLDPE (Exact 3128) at various extensional rates at 100 °C

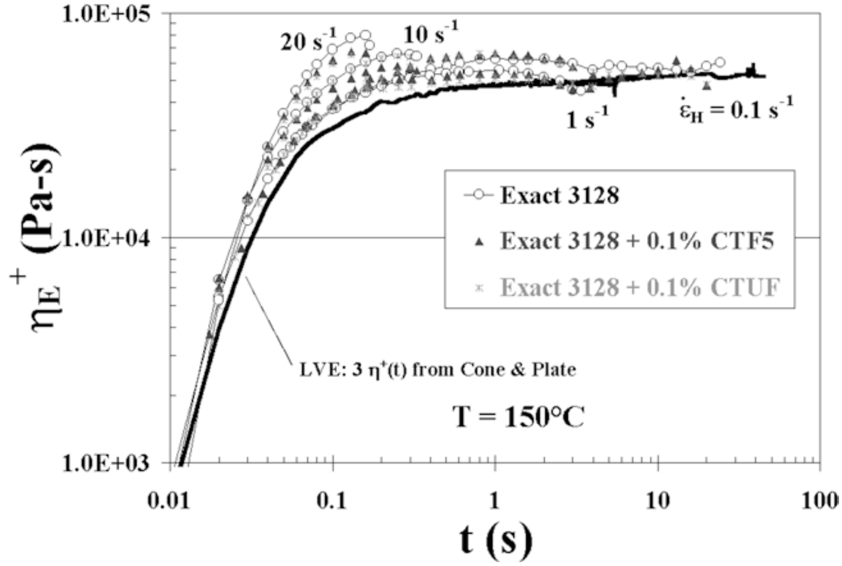

Fig. 8 Tensile stress growth coefficient at various extensional rates of boron nitride(CTF5 and CTUF) filled and unfilled Exact 3128 at 150 °C

ences are clearly evident in Fig. 9a,b, where the tensile stress growth coefficient is plotted at a Hencky strain rate of 20 s^{-1} at 100 °C and 150 °C respectively using a linear scale. Reduction in the extensional behavior of filled melts have also been reported previously; however, the reported effect was of smaller scale and at higher filler loadings (Kobayashi et al. 1995; Le Meins et al. 2003). The effects reported here appear to be more dramatic.

It appears that the extensional stress grows more rapidly in the absence of boron nitride prior to material rupture. The presence of CTF5 and CTUF significantly decreases the growth rate of extensional stresses by a factor of more than two at the lowest temperature, compared to the case of pure m-LLDPE (Exact 3128). The effects are more dramatic at 100 °C, because the Hencky strain rate of 20 s^{-1} corresponds to the rate prevailing at the entrance to the capillary rheometer when gross melt fracture is obtained at this temperature of extrusion. With increasing temperature, higher extensional rates are needed to obtain gross melt fracture and therefore the effect is not as dramatic for this same rate of extensional deformation. Similar results can be seen in Fig. 10for the case of the other m-LLDPE (Exceed 143). The presence of boron nitride (CTF5) causes a reduction in the extensional stress growth coefficient particularly at high extensional rates. This polymer exhibits gross melt fracture at rates much

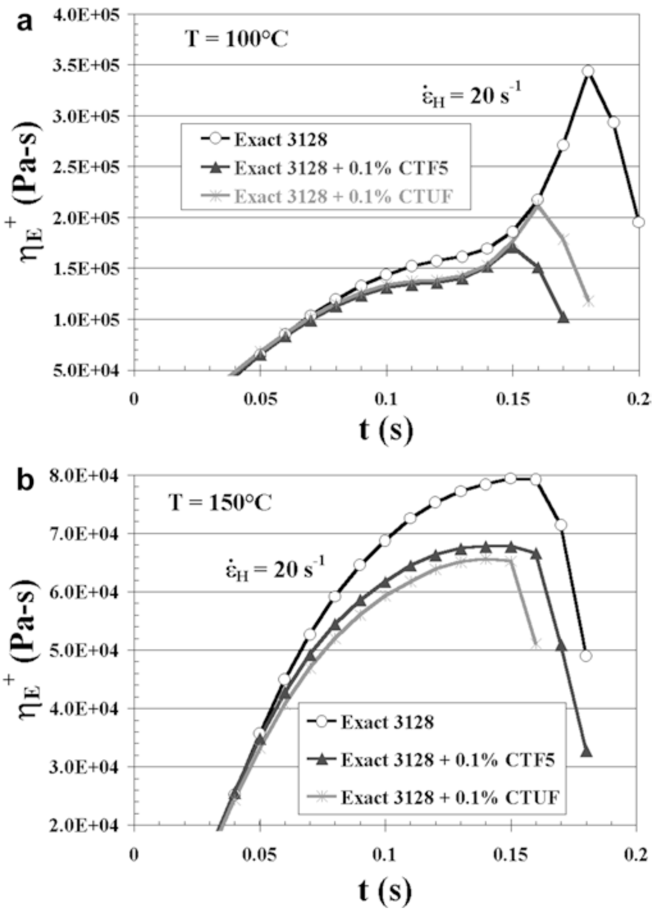

Fig. 9 a Tensile stress growth coefficient at 20 s^{-1} of boron nitride (CTF5 and CTUF) filled and unfilled m-LLDPE (Exact 3128) at 100 °C. **b** Tensile stress growth coefficient at 20 s^{-1} of boron nitride (CTF5 and CTUF) filled and unfilled m-LLDPE (Exact 3128) at 150 °C

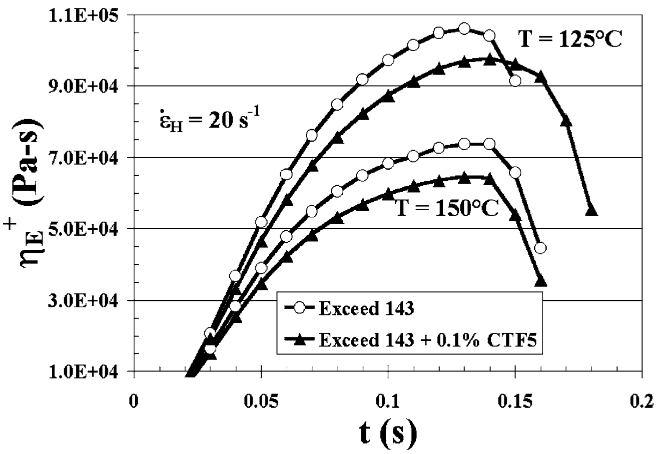

Fig. 10 Tensile stress growth coefficient of BN-filled and unfilled Exceed 143 at 125 and 150 °C at the rate of 20 s^{-1}

higher than those of Exact 3128 and therefore much higher extensional rates are needed in order to see a more dramatic reduction in the extensional stress growth coefficient in the presence of boron nitride.

According to these results, the addition of BN appears to stifle both the high rate and large strain deformation characteristics of the material as witnessed by the inherently lower rate of stress growth in this flow regime. This observation is most apparent by the data at 10 and 20 s^{-1} at 100 °C (about 8 °C above the melting point). The significant strain hardening exhibited by the virgin Exact 3128 polymer at this temperature near the melt state is attributed to strain induced crystallization which often occurs for linear polymer melts undergoing very large and rapid extensional deformations at rates near the melt temperature (Sentmanat 2003a). Hence, the significant difference in growth rate and strain hardening behavior for these polymers suggests that the presence of boron nitride has a deleterious effect on the crystallization kinetics of the polymer at this temperature and rate of deformation.

Furthermore, the results plotted in Figs. 7, 8, 9, and 10 suggest that boron nitride appears to behave as an energy dissipater, i.e., the energy that would normally be borne solely by the physical network of entanglements is now dissipated by the frictional interaction of the BN filler and the polymer chains. Figure 11 illustrates this proposed mechanism of energy dissipation. Figure 11a depicts the entrance region to the capillary die and the structure of flow under gross melt fracture conditions as described by Kazatchkov et al. (2000). Under such conditions the flow is broken down to several layers which flow and stop intermittently, thus producing a stick-slip pattern within the bulk of the polymer at several singular surfaces. This is due to the high extensional stresses that are generated as result of the storage of elastic energy when highly entangled polymer chains are rapidly stretched in the entrance region of the capillary die at high rates of flow. When the extensional stress is higher than the load which can be supported by the entanglements at certain surfaces, then the material fails catastrophically. This catastrophic failure has been described mathematically at a molecular level by Joshi and Denn (2003a, 2003b) for a polymeric filament in elongational flow. They have postulated that a catastrophic failure occurs when the frictional force on an entangled chain can no longer balance the tension in the chain.

However, when BN particles are present in the polyethylene (Fig. 11b), their presence disrupts the entanglement density of the polymer to a certain extent. Due to strong adsorption of polyethylene molecules on the surface of boron nitride the resistance to flow remains about the same (Rathod 2003). In other words, many entanglements have been substituted by BN par-

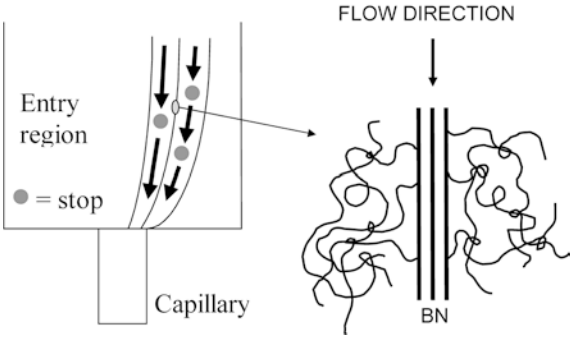

Fig. 11 Schematic illustration showing the proposed mechanism by which the presence of boron nitride reduces the extensional stress growth coefficient of polyethylenes

ticles, which connect molecules through adsorption. With a particle size of 10–20 μm, the flat plate-like surface of a BN particle can accommodate several polymer chains that are capable of "wetting" its surface in a somewhat "frozen" entropy state of chain configuration. As such these "wetted" chains sparingly participate in the overall bulk deformation of the polymer melt. As the extensional stresses in the bulk increase, the influence of the surrounding bulk polymer chains stimulates reconfiguration of the "wetted" polymer chains on the BN surfaces. In this manner, the energy that would normally be elastically stored by the bulk polymer chains approaching their limits of finite extensibility are somewhat dissipated by the frictional and reconfigurational motions of the wetted polymer chains sliding on the BN surface. Thus, for large rapid deformations, the stress at rupture for the BN filled polymer is less than for the virgin polymer. Hence, for strain governed events such as that which occurs in entrance die flow, the high extensional stresses normally borne by the virgin polymer are dissipated by the BN filled polymer in the form of isolated rupture or slip planes within the melt at the die entrance region as observed by Kazatchkov et al. (2000). These isolated rupture or slip planes subsequently "heal" upon entering the die.

Conversely, for stress governed events such as flows involving free surfaces, the ability to dissipate energy in the manner described is typically manifested in the form of increased extensibility. Therefore, with regard to surface melt fracture phenomena, it is believed that this energy dissipation mechanism may also alleviate the large extensional stresses generated on the surface of the extrudate upon exiting the die, while serving to plasticize and reduce the elasticity of the polymer at the free surface, where rupture might otherwise occur. Thus, the slight presence of an effective boron nitride powder appears to lead to a number of discrete sites for energy dissipation within the bulk polymer which may serve to rapidly and dramatically reduce the rate of stress growth near the surface of the exiting extrudate during high rates of extrusion thereby inhibiting the onset of localized surface melt rupture.

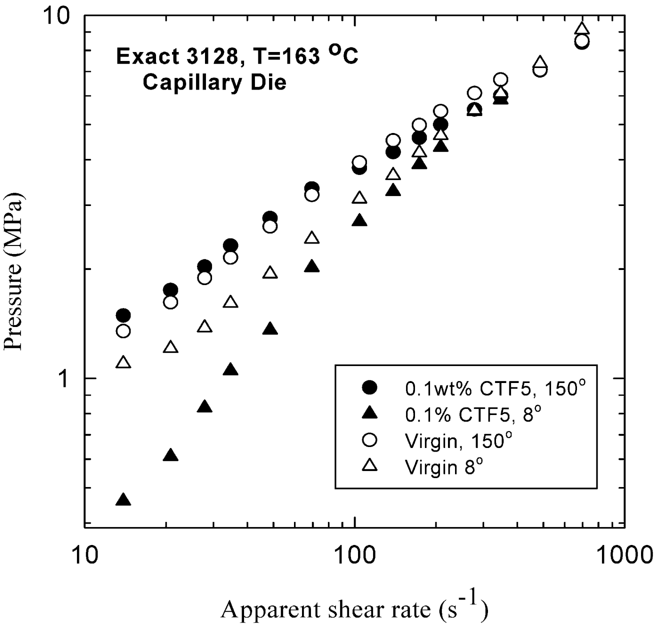

Fig. 12 Entrance pressure losses of m-LLDPE (Exact 3128) at two contraction angles of 8° and 150° at 163 °C

Returning now to gross melt fracture behavior, the rates at which these extensional rheological differences appear between filled and unfilled samples (Figs. 7, 8, 9, and 10) are relevant to the rates that prevail in the entrance to the capillary die when gross melt fracture appears. An approximate analysis to calculate these extensional rates is the one proposed by Cogswell (1972, 1977). In Cogswell's method, the average extensional rate, $\dot{\varepsilon}$, and extensional viscosity, $\eta_E(\dot{\varepsilon})$, as a function of end pressure, shear viscosity, η_S, and the local power-law exponent, n, are as follows:

$$\dot{\varepsilon} = \frac{4\dot{\gamma}_A^2 \eta_S}{3(n+1)\Delta P_{End}}, \eta_E(\dot{\varepsilon}) = \frac{9(n+1)^2(\Delta P_{End})^2}{32\eta_S\dot{\gamma}_A^2} \quad (3)$$

where the local power-law exponent, n, is determined locally from a shear stress versus apparent shear rate log-log plot.

In order to estimate the average extensional rates at the entrance to capillary relevant to gross melt fracture phenomena, the viscosity function as well the entrance pressure loss as a function of apparent shear rate are needed. Figures 3 and 4 plot the viscosity of m-LLDPE (Exact 3128) at 100 °C and 163 °C. Figure 12shows entrance pressure losses for the m-LLDPE (Exact 3128) at two different contraction angles, namely 8° and 150° at 163 °C. Note that the entrance pressure losses plotted vs shear stress are independent of temperature effects consistent with the time-temperature superposition principle. Therefore, these data can be used for our calculations at 100 °C as well. The effect of the addition of CTF5 in Exact 3128 is clearly shown at small contraction angles. This is due to lubrication effects that prevail only at small entrance angles. However, at high shear rates, where gross melt fracture is obtained these differences diminish (see Fig. 12) and the decrease of the extensional rates by the presence of CTF5 cannot be explained by the reduction of entrance pressure losses.

The experimental data of Figs. 3, 4, and 12 can be used now to calculate average extensional rates that exist in the capillary entrance region at conditions where gross melt fracture exist. It was discussed above that the critical shear rate for the onset of gross melt fracture of Exact 3128 at 163 °C was 450 s^{-1}. The viscosity of Exact 3128 at this rate is about 1.5 kPa-s. Using an entrance pressure loss of about 8 MPa at this rate, the average extensional rate calculated from Eq. (3) turns out to be about 30 s^{-1}. Therefore at 163 °C gross melt fracture occurs at average extensional rates of 30 s^{-1} and higher (this is the reason that at 20 s^{-1} the effect of boron nitride on the reduction of extensional stress is not as dramatic). At this rate, the extensional stress is about 3 MPa, that is certainly of the correct magnitude (Kim and Dealy 2002a, 2002b). Similarly, at 100 °C the calculated average extensional rates that are relevant to gross melt fracture regime which occurs at rates 327 s^{-1} and higher, again turn out to be about 20 s^{-1} and higher. Therefore, any effect that boron nitride has in eliminating gross melt fracture would be seen at extensional rates of 20 s^{-1} and higher. This is the reason that the effect of boron nitride in reducing the extensional stress at this rate is very dramatic (see Fig. 9).

It is noted at this point that these are only rough average estimates and perhaps the initiation of gross melt fracture occurs locally at a point where the local extensional rate might well exceed these average values. As discussed before in reference to Figs. 7, 8, 9, and 10, the effect of addition of boron nitride in polyethylene on the pure extensional behavior of polyethylene was seen at rates of 10 $s^{-1}$and 20 s^{-1}. At a given rate, the effect of boron nitride on the extensional rheology of polyethylenes is more pronounced at a lower temperature simply because gross melt fracture at a lower temperature occurs at a lower rate. The effects are expected to be stronger and more pronounced as the extensional rate increases.

Conclusions

The mechanism by which the addition of a small amount of boron nitride into a polyethylene eliminates gross melt fracture was studied. Simple elongational viscosity measurements at high extensional rates revealed that the presence of boron nitride decreases significantly the extensional viscosity of polyethylenes. The extensional rates at which these effects are present were found to be about the same with those at which gross melt fracture is obtained. These were calculated by a simple method using Cogswell's analysis. These extensional measurements have shown that the well dispersed boron nitride particles dissipate the release of energy resulting from isolated rupture or slip planes that originate at the entrance to the capillary. It is believed that this dissipation mechanism reduces the elastic storage of energy generated in the entrance region of the die thereby delaying the onset of gross melt fracture. This energy dissipation mechanism may also be responsible for the elimination of surface melt fracture that might otherwise appear as a result of the large localized extensional stresses generated on the surface of the extrudate upon exiting the die. Extensional measurements at high rates were also capable of distinguishing an effective boron nitride from an ineffective one. An effective boron nitride has a surface chemistry conducive to polymer adsorption as reflected by a proper balance of its polar and non-polar components.

Acknowledgement This work was financially supported by a strategic grant provided by NSERC Canada.

References

Achilleos EC, Georgiou G, Hatzikiriakos SG (2002) The role of processing aids in the extrusion of molten polymers. J Vinyl Addit Technol 8:7–24
Bagley EB, Schreiber HP (1961) Effect of die entry geometry on polymer melt fracture and extrudate distortion. Trans Soc Rheol 5:341–353
Ballenger TF, Chen I, Crowder J, Hagler GE, Bogue DC, White JL (1971) Polymer melt flow instabilities in extrusion. Trans Soc Rheol 15:195–215
Benbow JJ, Lamb P (1963) New aspects of melt fracture. S.P.E. Trans 3:7–12
Bergem N (1976) Visualization studies of polymer melt flow anomalies in extrusion. Proceedings of the 7th Congress on Rheology, Gothenberg, pp 50–54
Bird RB, Armstrong RC, Hassager O (1987) Dynamics of polymeric liquids. Wiley, NY
Buckmaster MD, Henry DL, Randa SK (1997) U.S. Patents 5,688,457 issued to E. I. DuPont de Nemours & Co Inc
Cogswell FN (1972) Converging flow of polymer melt in extrusion dies. Polym Eng Sci 12:64–73
Cogswell FN (1977) Converging flow and stretching flow: a compilation. J Non-Newtonian Fluid Mech 4:23–38
Done DS, Baird DG, Everage AE (1983) The influence of porous media on the flow of polymer melts in capillaries. Chem Eng Commun 21:293–309

Goutille Y, Guillet J (2002) Influence of filters in the die entrance region on gross melt fracture: extrudate and flow visualization. J Non-Newtonian Fluid Mech 102:19–36

Goutille Y, Majeste J-C, Francois Tassin J-F, Guillet J (2003) Molecular structure and gross melt fracture triggering. J Non-Newtonian Fluid Mech 111:175–198

Howells ER, Benbow JJ (1962) Flow defects in polymer melts. Trans Plast Inst 30:240–253

Hürlimann HP, Knappe W (1972) Der Zusammenhang zwischen der Dehnspannung von Kunststoffschmelzen im Düseneinlauf und im Schmelzbruch. Rheol Acta 11:292–301

Joshi YM, Denn MM (2003a) Rupture of entangled polymeric liquids in elongational flow. J Rheol 47:291–298

Joshi YM, Denn MM (2003b) Planar contraction flow with a slip boundary condition. J Non-Newtonian Fluid Mech 114:185–195

Kazatchkov IB, Yip F, Hatzikiriakos SG (2000) The effect of boron nitride on the rheology and processing of polyolefins. Rheol Acta 39:583

Kim S, Dealy JM (2002a) Gross melt fracture of polyethylene. I. A criterion based on tensile stress. Polym Eng Sci 42:482–494

Kim S, Dealy JM (2002b) Gross melt fracture of polyethylene. II. Effects of molecular structure. Polym Eng Sci 42:485–503

Kobayashi M, Kahahashi T, Takimoto J, Koyama K (1995) Flow-induced whisker elimination and viscosity for molten composite systems in a uniaxial elongational flow-field. Polymer 36:3927–3933

Kurtz SJ (1992) The dynamics of sharkskin melt fracture: effect of die geometry. Proceedings of the 11th International Congress on Rheology. In: Moldenaers P, Keunings R (eds) Theoretical and applied rheology. Elsevier Science Publishers, Brussels, p 377–379

Larson RG (1992) Instabilities in viscoelastic flows. Rheol Acta 31:213–263

Lee SM, Lee JW (2001) The effect of boron nitride on the rheological properties and processability of polyethylene. ANTEC '2001, Society of Plastics Engineers, New York, NY, USA, vol 45, pp 1223–1227

Lee SM, Kim JG, Lee JW (2000) The effect of boron nitride on the processability of metallocene based LLDPE. ANTEC '2000, Society of Plastics Engineers, New York, NY, USA, vol 46, pp 2862–2866

Le Meins J-F, Moldenaers P, Mewis J (2003) Suspensions of monodisperse spheres in polymer melts: particle size effects in extensional flow. Rheol Acta 42:184–190

Leonov AL, Prokunin AN (1994) Nonlinear phenomena in flows of viscoelastic polymer fluids. Chapman and Hall, NY, pp 356–396

Migler KB, Lavallee C, Dillon MP, Woods SS, Gettinger CL (2001) Visualizing the elimination of sharkskin through fluoropolymer additives: coating and polymer-polymer slippage. J Rheol 45:565–581

Migler KB, Son Y, Qiao F, Flynn K (2002) Extensional deformation, cohesive failure and boundary conditions during sharkskin melt fracture. J Rheol 46:383–400

Pearson JRA (1985) Mechanics of polymer processing. Elsevier, London

Piau JM, Nigen S, El Kissi N (2000) Effect of die entrance filtering on mitigation of upstream instability during extrusion of polymer melts. J Non-Newtonian Fluid Mech 91:35–57

Ramamurthy AV (1986) Wall slip in viscous liquids and influence of materials of construction. J Rheol 30:337–357

Rathod N (2003) The effect of surface properties of boron nitride on the processability of polymers. M.A.Sc. Thesis, The University of British Columbia, Vancouver, Canada

Rosenbaum EE, Randa S, Hatzikiriakos SG, Stewart CW (2000) Boron nitride as a processing aid for the extrusion of polyolefins and fluoropolymers. Polym Eng Sci 40:179–190

Sentmanat ML (2003a) A novel device for characterizing polymer flows in uniaxial extension. ANTEC '03, Society of Plastics Engineers, Tech Papers 49, CD-ROM, New York

Sentmanat ML (2003b) Dual windup extensional rheometer. US Patent No 6,578,413

Shaw MT (1975) Flow of polymer melts through a well-lubricated, conical die. J Appl Polym Sci 19:2811–2816

Tordella JP (1956) Fracture in the extrusion of amorphous polymers through capillaries. J Appl Phys 27:454–458

Tordella JP (1969) Unstable flow of molten polymers. In: Eirich FR (ed) Rheology, theory and applications. Academic Press, NY, pp 57–92

Vinodradov GV, Malkin AY (1980) Rheology of polymers, 1st edn. Moscow, Mir Publishers, Berlin: Springer, Berlin Heidelberg New York, pp 140–150

Yip F (1999) The effect of boron nitride on the rheology and processability of molten polymers. M.A.Sc. Thesis, The University of British Columbia, Vancouver, Canada

Yip F, Rosenbaum EE, Randa SK, Hatzikiriakos SG, Stewart CW (1999) The effect of boron nitride type and concentration on the rheology and processability of molten polymers. ANTEC '99, Society of Plastics Engineers, Tech Papers 45, New York, pp 1223–1227

Yip F, Rosenbaum E, Hatzikiriakos SG (2000) Boron nitride powders: new processing aids for molten polymers. J Plastic Film Sheeting 16:16–32